water

MDPI

Article

Influence of Dam Breach Parameter Statistical Definition on Resulting Rupture Maximum Discharge

Diego Bello [1], Hernán Alcayaga [1,*], Diego Caamaño [2] and Alonso Pizarro [1]

[1] Escuela de Ingeniería en Obras Civiles, Universidad Diego Portales, Santiago 8370109, Chile; diego.bello@mail.udp.cl (D.B.); alonso.pizarro@mail.udp.cl (A.P.)
[2] Departamento de Ingeniería Civil, Universidad Católica de la Santísima Concepción, Concepción 4030000, Chile; dcaamano@ucsc.cl
* Correspondence: hernan.alcayaga@udp.cl

Abstract: However rare, dam breach occurrences are recently reported and associated with significant damage to life and property. The rupture of the structural dam wall generates severe flow rates that exceed spillway capacity consequently generating unprecedented flooding scenarios. The present research aims to assess the influence of the dam breach statistical configuration on the most relevant parameters to predict the rupture maximum discharge (RMD). McBreach© software was used to provide the necessary inputs for the operation of the HEC-RAS dam breach module. McBreach© automates the process of batch mode simulations providing a Monte Carlo approach to characterize the breach parameters stochastically. Thus, a sensitivity analysis was performed to identify the most influential breach parameters, followed by an uncertainty assessment regarding their statistical definition of the resultant RMD. Analysis showed that the overtopping failure mode discharges are most sensitive to the breach formation time (tf) parameter, followed by the final height breach (Inv) and the final width of the breach (B), which combined are responsible for 85% of the rupture's maximum discharge. Further results indicated highly variable RMD magnitudes (up to 300%) depending on the breach parameter's statistical definition (i.e., probability density function and associated statistical parameters). The latter significantly impacts the estimated flood risk associated with the breach, the flood zone delimitation, preparation of emergency action plans (EAP) and scaling of future dam projects. Consequently, there is a plausible need for additional investigations to reduce this uncertainty and, therefore, the risk associated with it.

Keywords: dam breach; rupture maximum discharge; statistical definition

Citation: Bello, D.; Alcayaga, H.; Caamaño, D.; Pizarro, A. Influence of Dam Breach Parameter Statistical Definition on Resulting Rupture Maximum Discharge. *Water* **2022**, *14*, 1776. https://doi.org/10.3390/w14111776

Academic Editors: Francesca Aureli, Andrea Maranzoni and Gabriella Petaccia

Received: 5 May 2022
Accepted: 28 May 2022
Published: 1 June 2022

1. Introduction

Dams are used worldwide owing to their extensive contribution to the management of water demand in cities, agriculture, industry, power generation, and flood management. However, it is known that dams have a potential risk of failure [1]. A dam breach scenario involves the rapid evacuation of enormous volumes of water and sediment, which are associated with aggressive floods, economic losses, environmental damage, and the possible loss of human life. An example of this occurred in 1975 in Henan, China, where a five-day storm generated 1631 mm of rainfall that led to the overtopping of two large dams (Banqiao and Shimandan), two medium dams (Tiangang and Zhugou), and 58 small dams. For the Banqiao reservoir, a peak breach flow of 78,100 m^3/s was reached, resulting in inundations totaling 12,000 km^2, a death toll of more than 26,000, and economic losses exceeding USD 1.6 billion [2].

Based on the evidence, it is crucial to know the combination of possible hydrographs generated in a failure scenario. In these terms, the traditional way of conducting a dam breach analysis consists of three phases: (i) Hydraulic simulations of the dam breach; (ii) Deterministic analysis of breach parameters to model the hydrograph that would be

generated from the rupture; and, (iii) A hydraulic model to route the flood downstream. As established in the FEMA Guide [3], there are a series of mathematical models and methods for analyzing each of these three phases. It is important to indicate that dam breach simulations are designed to predict the resulting flood hydrograph and not the moment of failure [4]. This prediction would be highly sensitive to the in situ conditions (dam and field conditions) because a wide range of possible alternatives are physically valid in classifying the required modeling parameters. Therefore, determining breach parameters usually involves reviewing and evaluating parametric regression equations, revising probable failure mode reports, and expert judgment [5]. The latter is generally associated with a significant level of uncertainty [6,7].

Faced with this problem, many studies have investigated different methods for reducing this uncertainty [8–14]. For example, Pierce [13] used a series of existing equations and empirical methods to assign values to the breach parameters (e.g., breach width and breach formation time). This type of approach is usually based on the analysis of observed data from existing dam failures, such as the analyzes performed by Wahl [7,15]. Despite these efforts, deterministic models fail to adequately incorporate the process of dam breaches because they do not consider critical factors such as the randomness of a natural system, the limitations of the modeling approach, and possible errors in the observed data [16]. The challenge for engineers and scientists is to use statistical approaches to make more accurate estimates from limited data sets [17]. In this context, probabilistic methodologies have been proposed to quantify the associated uncertainty. Among them, Goodel [18] states the importance of knowing the uncertainty related to hydraulic models for flood risk studies and mentions the approaches to risk analysis established in different continents such as Africa [14], Europe [19], Asia [20], and North America [3]. The latter quantified the effect on the RMD results given several models fed by different magnitudes of the breach parameters, making it possible to assign probabilities of occurrence to the results and thus determine flood risks [16].

Despite significant efforts in this regard, some questions remain unanswered [21]. One of the most important gaps in the literature is related to the sensitivity of the solution with respect to the required parametrizations. The latter can be posed as a function of questions that are briefly mentioned as follows: (i) Which breach parameters have the most significant weight for any given case? (ii) How does the parameter's statistical definition affect the rupture's maximum discharge (RMD)? (iii) Does this characterization affect the peak flow in the same way that it affects the shape of the hydrograph? Given the above open questions, the main goal of this paper is to determine the sensitivity of the RMD with respect to the most relevant parameters required for the dam breach simulation.

The rest of the paper is organized as follows: Section 2 presents the methodology used for the hydraulic simulations (using McBreach and HEC-RAS); the Chacrillas case study; and the different configurations for the sensitivity analysis. Section 3 shows the results, highlighting the breach parameters that have the most significant influence on the RMD and the influence of statistical parameters, respectively. Conclusions are provided at the end.

2. Methods

2.1. Workflow Adopted

Hydraulic simulations were performed using the United States Army Corp of Engineers software HEC-RAS v5.0.7 (Hydrologic Engineering Center's, CEIWR-HEC, Davis, CA, USA) [22]. In contrast, a Monte Carlo approach provides the required breach parameter characterization using the software package McBreach© v5.07 (Pittsfield, ME, USA) by Kleinschmidt [23].

The dam failure mode addressed in the present study corresponds to overflow or overtopping. This type of failure occurs when the water surface elevation in the reservoir exceeds the dam's height, with water flowing through the upper ridge until it causes the wall to break, culminating in the evacuation downstream of a volume of water of great

magnitude. The overflow implies that the weir system of the dam is not working properly, or there is more water than the designed spillway capacity. The overtopping failure mode is the one that occurs most frequently in the different types of dams [24] and the Concrete-face Rockfill Dam (CFRD) is the type of dam widely used around the world [3]

HEC-RAS is equipped with a dam break module that uses nine breach parameters. These parameters can be grouped according to their characteristics: (i) three geometric parameters (width of the breach, slopes of the breach and final height of the breach); (ii) one to define the breach formation time; and (iii) five parameters to characterize the breach flow (discharge coefficient, height of the breach, tolerable height of the water before a failure occurs, weir coefficient and height where internal erosion begins) [25]. HEC-RAS simulates the overflow discharge over the dam as a flow over a weir. Then, to measure the magnitude of the overflow discharge, three variables are used: (i) the weir discharge coefficient; (ii) the hydraulic head; and (iii) the crest length, with the last two representing functions of time [22]. Seven of the above-mentioned breach parameters describe the overtopping failure mode in HEC-RAS (see Table 1 for definitions and abbreviations of variables).

Table 1. Dam breach parameters used by HEC-RAS when overtopping is considered.

Overtopping Breach Parameters in HEC-RAS	Abbreviation
Final breach height	Inv [m.s.n.m]
Final breach width	B [m]
Left side slope of the breach	LSS [H:V]
Right side slope of the breach	RSS [H:V]
Breach formation time	tf [h]
Height of the water for failure to occur	Init [m.s.n.m]
Discharge coefficient	Cd

Many combinations of these variables can be met in field conditions causing different scenarios. The randomness of the parameter combinations is conditioned by probability density functions, which in turn are characterized by statistical parameters (i.e., mean, standard deviation and mode). Four different distribution functions are considered in McBreach, and the statistical parameters that define them are presented in Table 2. The physical range of operation of each breach parameter is identified based on empirical equations such as those proposed by [7,13] combined with the in situ conditions of the studied dam (e.g., the final breach width cannot exceed the width of the wall crest, which defines the maximum magnitude). The given magnitude for each simulation is provided by a Monte Carlo approach, which through many iterations of complex calculations, obtains a statistically valid result [26]. The minimum number of simulations that allows the statistical convergence of the data (i.e., an optimal sample size) corresponds to 10,000 breach parameter combinations. Thus, McBreach© calculates 10,000 simulations of the HEC-RAS dam breach model for each statistical scenario.

Table 2. Statistical indicators and distribution functions available in McBreach.

Statistical Distribution Functions	Statistical Parameter
Uniform	NA
Triangular	Mode
Normal	Mean and standard deviation
Log-Normal	Mean and mode

The probabilistic analysis results were used to generate a series of scenarios to quantify the uncertainty associated with the combination of the breach parameters and the RMD. This allowed the variability of the generated peak breach flows to be analyzed following the hydraulic and probabilistic model simulations. Figure 1 illustrates the stages used in the uncertainty and sensitivity analyzes, which are treated in detail below.

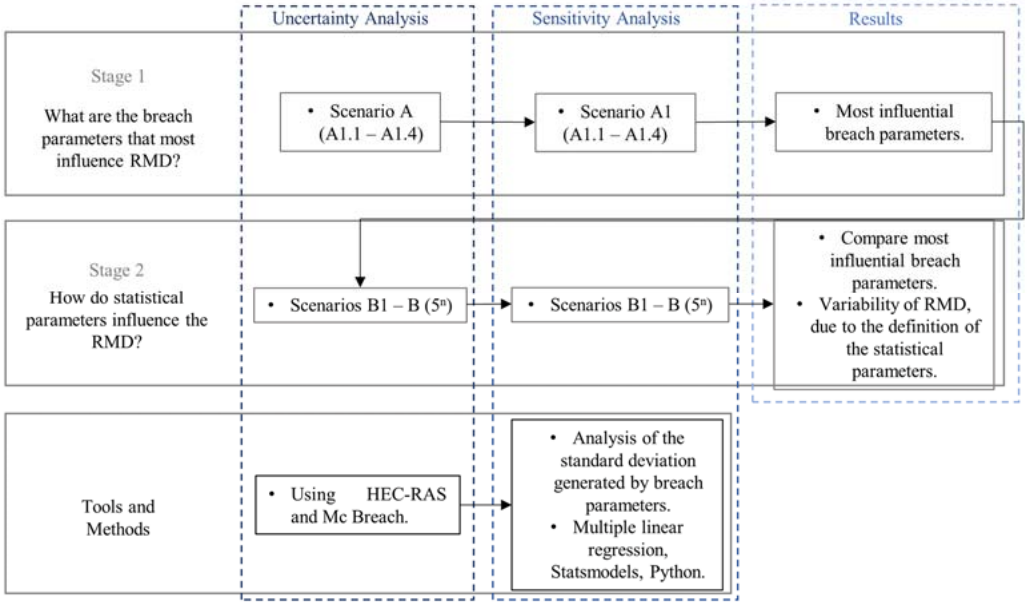

Figure 1. Illustration of the workflow adopted in this paper.

Although research has been conducted on the selection of breach parameters [8–14], the probability distributions that best fit these parameters and the associated uncertainty are generally unknown. Despite this matter, the normal distribution is usually adopted for uncertainty and sensibility analyses [18,27,28]. This work aligns with the former assumption, and Table 3 shows the statistical parameters for the base case.

Table 3. Statistical parameter values for the base case.

PDF	Statistical Parameter	Inv [m.s.n.m]	B [m]	LSS	RSS	Tf [h]	Init [m.s.n.m.]	Cd
Normal	Mean	1272	31.50	0.80	0.80	1.55	1338.85	2.80
	Standard deviation	9.30	7.80	0.26	0.26	0.48	0.11	0.06

Furthermore, six sub-scenarios were established with the base case distribution but with different statistical parameters to analyze the mean and standard deviation sensibility. These sub-scenarios change the mean and the standard deviation by 50% (i.e., +50% of the mean value; −50% of the mean value; +50% of the standard deviation; −50% of the standard deviation; +50% of both the mean value and standard deviation; and −50% of both the mean value and standard deviation). The variability of the RMD against the magnitude of statistical parameters and influential breach variables was also determined. In this case, the number of scenarios was determined by the expression 5^n, where the number 5 represents the sets of statistical parameters varying from a base value and ranging −50% to +50% with 25% intervals (i.e., −50%, −25%, base value, +25%, and 50%). Whereas "*n*" is the number of breach variables established as probabilistic in McBreach. Therefore, B1 to B(5n) scenarios are generated.

Worthy of mentioning is that the breach parameters—having less influence on the RMD—were assumed with a constant value in McBreach. Consequently, their influence was considered deterministic (their values were fixed by the combination of breach parameters associated with an RMD with an exceedance probability of 50%). An exceedance probability of 50% was selected because the magnitude of the RMD generated by the combination of the breach parameters was found at the middle rather than the upper or lower extremes.

2.2. Case Study: The Chacrillas Reservoir

The defined methodology was applied to the Chacrillas Reservoir in the Andes Mountains of central Chile (70°30′ W, 32°30′ S). Its wall is located 2.5 km upstream of the confluence of the Rocín River and Chalaco Estuary (Figure 2). The delimited reservoir basin has a surface area of 630 km^2. Downstream from the Chacrillas Reservoir wall (Figure 2b), the Rocín River has a 1.8% longitudinal slope and a gravel bed (d_{50} = 14 mm). The most important urban settlement is the town of Putaendo (around 17,000 inhabitants), located 13 km upstream from the confluence of the Putaendo and the Aconcagua Rivers. The average annual precipitation in the basin is 307.7 mm (according to the Resguardo de los Patos station, maintained by the Chilean organization in charge). The hydrological regime is nivo-pluvial with an average annual flow of 1.19 m^3/s. The dam wall is of Concrete Face Rockfill Dam type, and its construction began in 2011 and ended in 2017 [29]. The construction characteristics of the Chacrillas Reservoir wall are presented in Table 4.

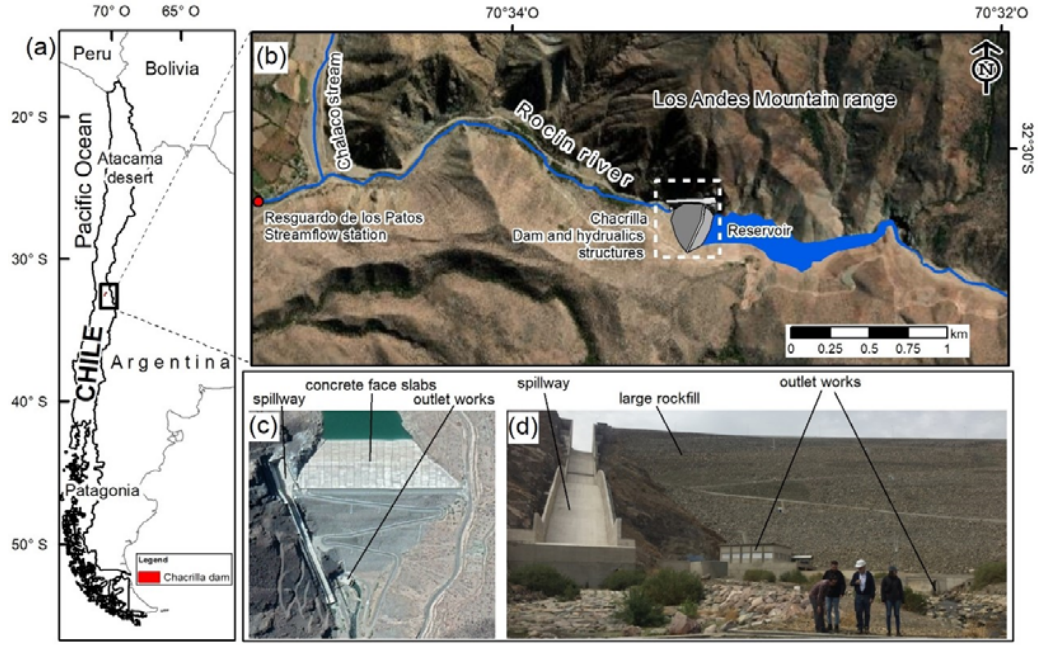

Figure 2. (**a**,**b**) Location of the Chacrillas Reservoir; (**c**) Zoom of the Chacrillas Reservoir with outlet works and concrete face slabs; (**d**) Zoom of the spillway.

Table 4. Characteristics of the Chacrillas dam.

Dam Element	Value	Unit
Crest height	1338.5	m.s.n.m
Crest length	319	m
Crest width	10	m
Dam height	102.5	m
Reservoir capacity	31	Hm^3
Regulation volume	27	Hm^3
Maximum water level	1337.5	m.s.n.m
Minimum water level	1264	m.s.n.m
Upstream slope	1.5:1	H:V
Downstream slope	1.6:1	H:V

A one-dimensional (1D) hydraulic model was created for a non-steady flow, where the hydrograph influencing the reservoir—with a Probable Maximum Flood of 2770 m^3/s—was considered as the upstream boundary condition [21]. Downstream, the geometric characteristics of the Rocín River channel (i.e., the shape of the cross-sections without

abrupt changes, stable longitudinal slope, and homogeneous roughness) suggest a downstream boundary condition established by the normal depth. The topography used for the modeling was the same as that used to design the reservoir, contemplating 4.5 km upstream of the dam and up to 1 km downstream (Figure 2b). The spatial discretization adopted was 10 m between cross-sections, which allowed the definition of the calculation time step to satisfy the Courant numerical stability criteria [22].

Table 5 shows the range of magnitudes defined for each breach parameter based on empirical equations proposed by [7–13], and adjusted to the characteristics of the Chacrillas in situ conditions. This configuration was used in each of the simulations conducted with McBreach.

Table 5. Range of breach parameters for the probabilistic model.

Inv [m.s.n.m]	B [m]	LSS	RSS	tf [h]	Init [m.s.n.m]	Cd
1244–1300	8–55	0–1.6	0–1.6	0.1–3.0	1338.82–1339.82	2.6–3.0

3. Results

The uncertainty that exists when determining the magnitude of the RMD was quantified for each combination of breach parameters in each of the sub-scenarios. Figure 3 shows the variability in the magnitude of the peak breach flows with respect to the variation of the statistical parameters that define the distribution (mean and standard deviation). The curve with the largest flows corresponds to scenario A2, where a 50% decrease in the mean value was considered. The curve with the smallest magnitudes in its peak breach flows is scenario A1, corresponding to a 50% increase from the mean. As shown in the A sub-scenarios, the mean has a greater weight than the standard deviation on the results of the RMD calculation.

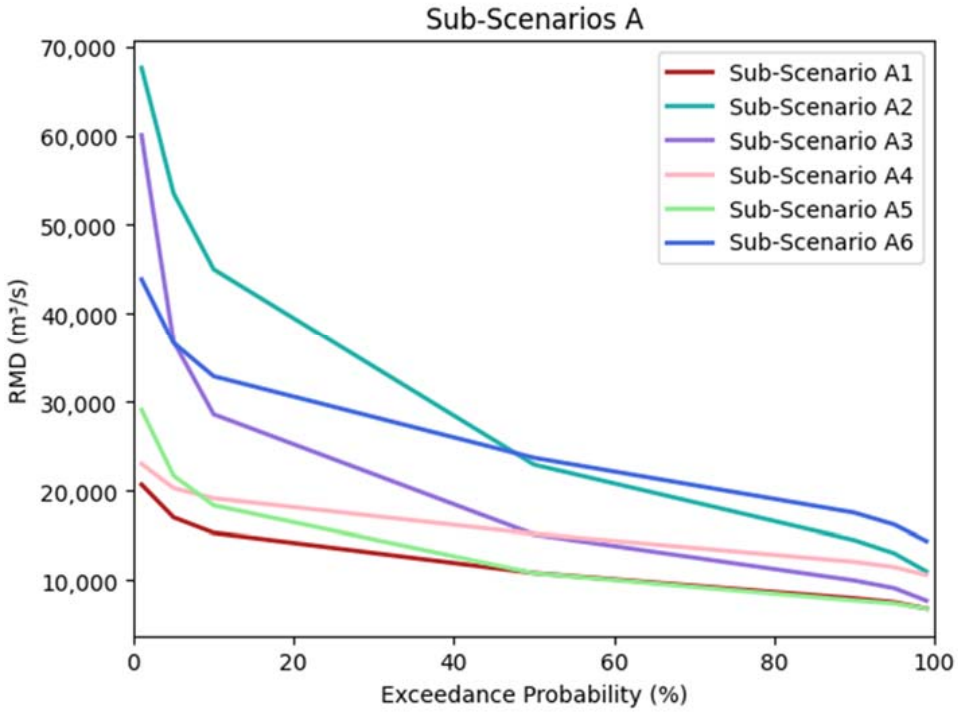

Figure 3. RMD exceedance probability curves for A2 scenarios.

Despite being able to visualize certain variations in the magnitude of the RMD, it is not possible to relate this variability to a specific breach parameter. To identify the parameter(s) that were most relevant to the calculation of the RMD, the sensitivity analysis described below was performed.

3.1. Sensitivity Analysis

Following the scatter plot analysis procedure described in [30], the standard deviations of the peak flows were calculated. In Figure 4, the results of these standard deviations are presented as a function of the breach parameters. It is evident that the breach parameter with the highest standard deviation value and, therefore, the greatest influence on the RMD calculation is the breach formation time (tf). Given that the order of breach parameter importance is different according to the scenario, we could not define at this point which parameters were the most influential with respect to the RMD after tf. For this reason, Multiple Linear Regressions (MLR) were performed for each sub-scenario to understand the variability of the relationship that exists between breach parameters (predictors) and the RMDs (response variable).

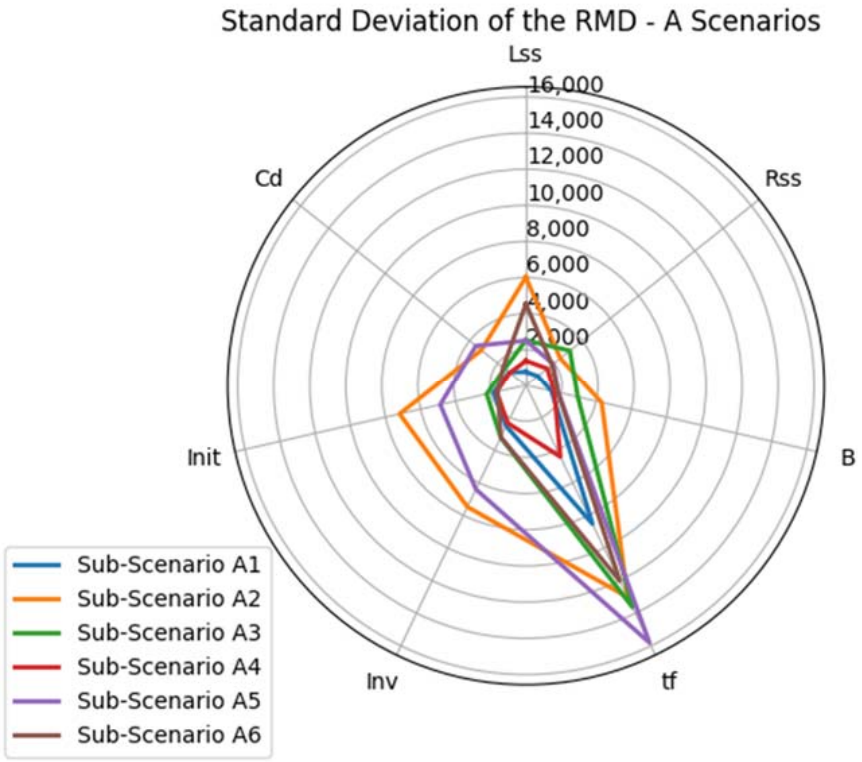

Figure 4. Standard deviation of the RMD produced by each breach parameter for A sub-scenarios.

MLR were performed between 10,000 combinations of simulated breach parameters and their respective RMDs for each scenario using Python's Statsmodels module [31]. The MLR allowed the obtention of several coefficients (Bj), which represent the weight of each parameter compared to the RMD. In Equation (1), the relationship between the coefficients, the breach parameters and the RMD is shown.

$$\begin{aligned} RMD = Bj_{Inv} \times Inv^* + Bj_B \times B^* + B_{jLSS} \times LSS^* + B_{jRSS} \times RSS^* + Bj_{tf} \times\ tf^* \\ \times Init^* + Bj_{Cd} \times Cd^* + e \end{aligned} \quad (1)$$

where the coefficients (Bj) represent each breach parameter, the RMD is measured in m^3/s and "e" represents the residual of the MLR. Worthy of mentioning is that all the breach variables were normalized before fitting Equation (1) (e.g., $Inv^* = Inv/Inv_{max}$).

The results of the MLR analysis are shown in Figure 5. The values correspond to the coefficients of the predictors of the MLR of each sub-scenario, representing the average change expected for the response variable (RMD) by increasing the predictive variable (breach parameters) by one unit. The graphs confirm that the parameter to which the RMD is most sensitive is tf. In addition, it clearly shows that the most influential breach

parameters after tf are Inv and B, respectively, and that the remaining four parameters (LSS, RSS, Init and Cd) have little relevance in determining the RMD.

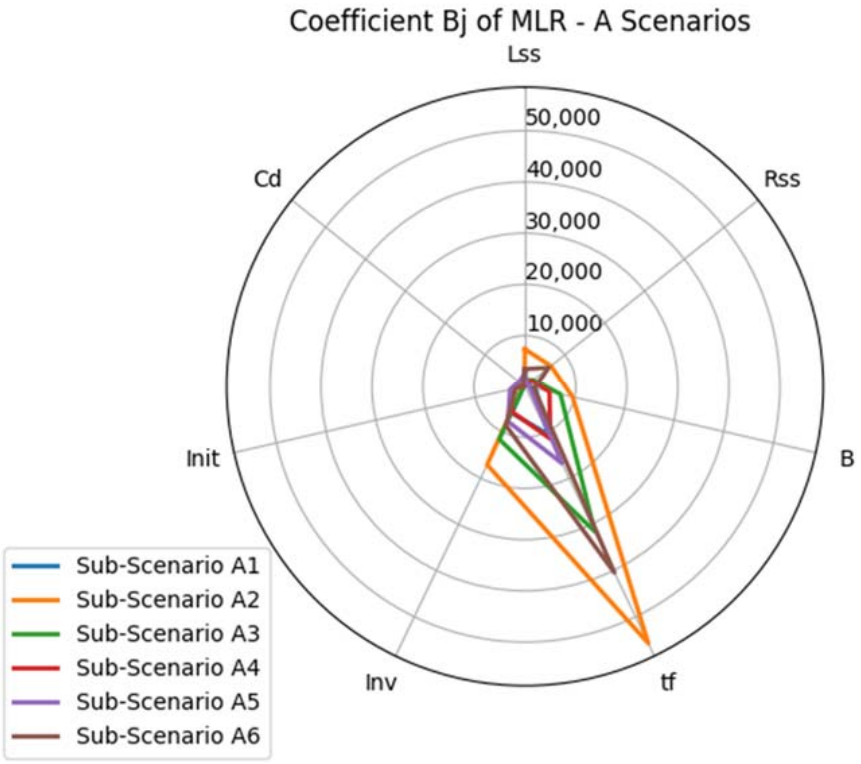

Figure 5. Coefficients of the predictors for the sub-scenarios.

Following these results, a distinction was made between the breach parameters to minimize computational costs while capturing the main dynamics of the process. As only three variables were the most influential ones, they were defined as probabilistic parameters in McBreach. Therefore, 125 scenarios (5^3) were generated. For these three parameters defined as probabilistic, five sets of statistical parameters (mean and standard deviation) were established, as seen in Table 6. The percentage variations were applied to the base condition of the normal distribution presented in Table 3.

Table 6. Stage 2 statistical parameter set.

Most Influential Breach Parameter with Respect to RMD	Mean [%]	Std. Deviation [%]
tf, Inv, B	+50	+50
	+25	+25
	Base condition	Base condition
	−25	−25
	−50	−50

The combinations of breach parameters and statistical parameters (mean and standard deviation) that characterize the normal distributions associated with the 125 scenarios are presented in the supplementary material (Table S1: Combinations of statistical parameters. Table S2: Combinations of statistical and deterministic parameters. Table S3: Combinations of breach parameters).

Consequently, since the LSS, RSS, Init and Cd parameters were found to have a low influence on the RMD, they were considered deterministic and were defined based on the combination of breach parameters which generated an RMD with an exceedance probability of 50% (Table 7).

Table 7. Combination of breach parameters associated with an RMD with an exceedance probability of 50% for sub-scenario A1.3.

Exc. P 50% Sub-Scenario A1.3	Inv [m.s.n.m]	B [m]	Tf [h]	LSS	RSS	Init [m.s.n.m]	Cd	Qmax [m^3/s]
	1272.39	32.06	1.91	1.07	0.66	1338.82	2.83	11,575

3.2. Uncertainty Analysis

The exceedance probability curves for the RMD were obtained from the results of the 125 simulations in McBreach (Figure 6). This allowed the uncertainty associated with using the probabilistic parameters that generated these flows to be quantified. The results showed that for the exceedance probability of 99%, the highest and lowest flows obtained correspond to approximately 17,000 m^3/s and 6000 m^3/s, respectively. Furthermore, the variation is almost three times greater due to the value defined for the mean and standard deviation, demonstrating the enormous importance of selecting these probabilistic parameters. For the exceedance probability of 1%, the highest and lowest flows reached an approximate magnitude of 60,000 m^3/s and 22,000 m^3/s, respectively, maintaining the same variation indicated above (i.e., almost three times). The curve that represents the most extraordinary magnitude flows (i.e., Max in Figure 6) corresponds to sub-scenario B121 (variation of −50% of mean and standard deviation to the base case for tf and Inv, and +50% of mean and standard deviation to the base case). Sub-scenario B5 had the lowest mean and standard deviation value of tf and Inv of the entire set of sub-scenarios and the highest mean and standard deviation of B for the entire simulated set. This is coherent since the RMD is inversely proportional to tf and Inv, and directly proportional to B. The curve representing the lowest magnitudes of RMD (i.e., Min in Figure 6) corresponds to sub-scenario B5, which is the opposite sub-scenario of B121. Sub-scenario B5 has a variation of +50% of mean and standard deviation to the base case for tf and Inv, and −50% of mean and standard deviation to the base case for B; that is, it has the highest mean and standard deviation values for tf and Inv, and the lowest mean and standard deviation values for B.

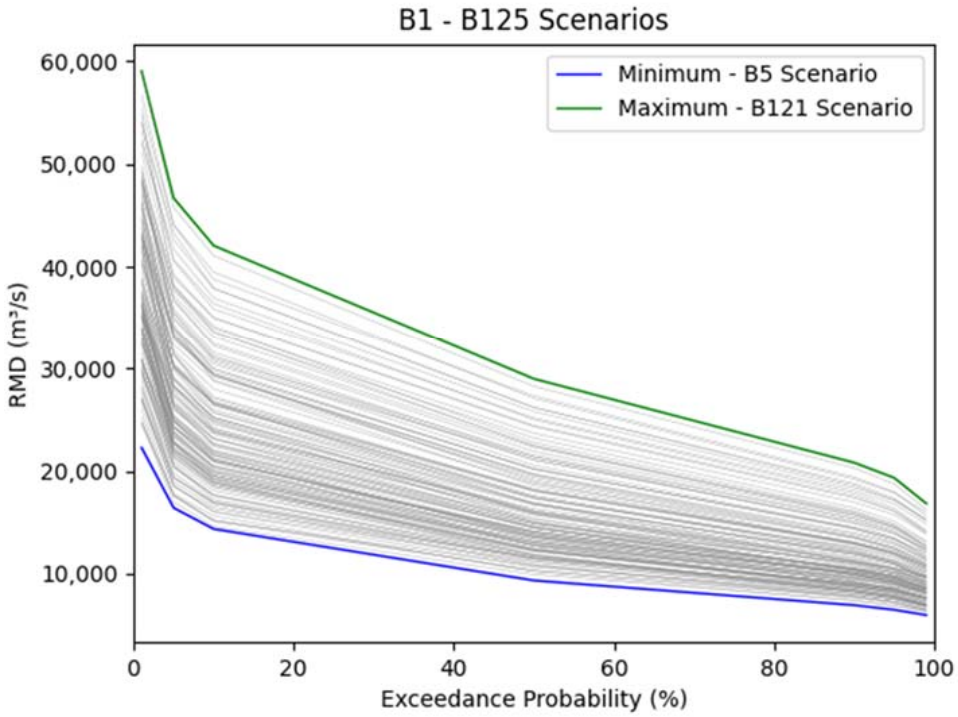

Figure 6. Exceedance probability curves and RMD for scenarios B1 to B125.

Figure 7 shows the calculated standard deviations of the breach parameters tf, Inv and B (Figure 7a), and the coefficient values of the predictors for the MLR (Figure 7b) for the 125 sub-scenarios of Stage 2. Regardless of the simulated scenario, the highest standard deviation of the RMD always corresponded to the parameter tf, and its magnitude was also much higher than that of the breach parameters Inv and B. The results of the MLR, which are expressed through the predictive coefficients Bj, clearly show that tf is the breach parameter that has the most significant influence on the RMD calculation. The parameter that has the second most influence in determining the RMD corresponds to Inv, while the third most influential parameter is B.

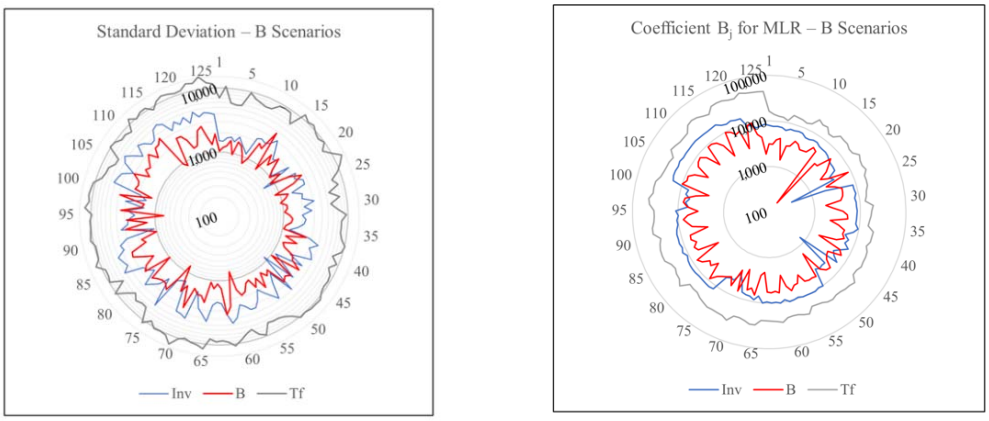

(**a**) (**b**)

Figure 7. (**a**) Standard deviation of the RMD produced by each breach parameter for B sub-scenarios; (**b**) Coefficients of the predictors for the B sub-scenarios.

After determining the order of the breach parameters with the most significant weight in the RMD calculation, the relationship between the magnitude of the statistical parameters (mean and standard deviation) with respect to the RMD was analyzed. For the analysis, the extreme values of the RMD were used (exceedance probabilities of 99% and 1%) so that all possible variations of the RMD were captured. Figure 8 shows the results of this analysis for the exceedance probabilities of 99% and 1%, as well as the means of the parameters tf, Inv and B (Figure 8a,b, respectively).

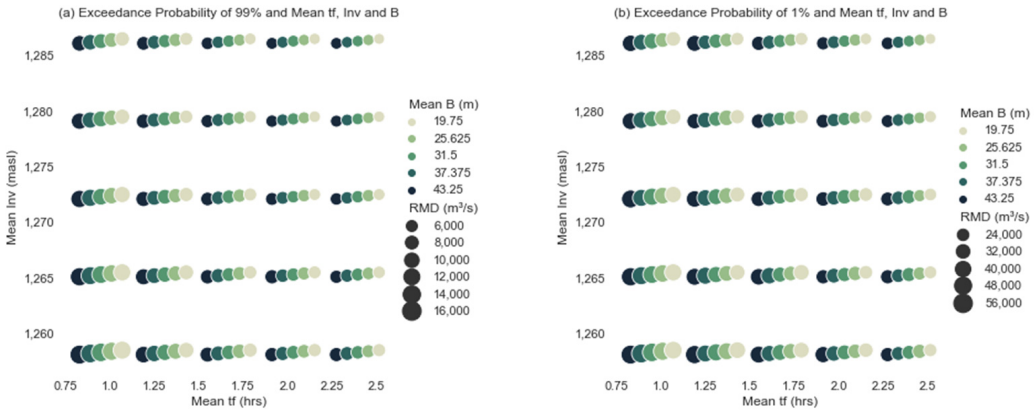

Figure 8. (**a**) Exceedance probability of 99% and mean tf, Inv and B; (**b**) Exceedance probability of 1% and mean tf, Inv and B.

Figure 8a,b show the relationship between the proportionality of the breach parameters (tf, Inv and B) indicated above and the definition of the statistical parameters (the mean, in this case). The set of results in the lower-left corner represents the RMDs with the highest

magnitudes of the 125 scenarios. In contrast, the set of results in the upper right corner of the graphs represents the opposite, corroborate what was expected.

As a function of the variation in the magnitude of the RMD, we can see that the Inv parameter is more influential than B, since the proportion by which the diameter of the circumference decreases as Inv increases is greater than compared to B. Continuing with the same analysis, the mean of the parameter tf changes along the horizontal axis of the graph, reaching the greatest magnitude flows with the lowest value of tf, with the magnitude decreasing as the mean increases. The radius of the circumference, which represents the proportion by which the magnitude of each flow decreases, is much greater than that displayed for Inv and B, corroborating that tf is the most influential of the three parameters.

For the graphs of each standard deviation associated with the flow magnitudes, the same results described above were obtained since the variation of the set of parameters considered the mean and the standard deviation as the same data set. Therefore, the variation results in the same percentage since the same flow magnitudes would be plotted with the same distribution as in Figure 8 but with the standard deviation values instead of the mean.

4. Discussion and Conclusions

The uncertainty associated with the magnitude of the breach hydrograph resulting rupture maximum discharge (RMD) was clearly shown in the results obtained in Stage 2, where for the same distribution analysis, a difference of three times was obtained for the exceedance probabilities of 99% and 1%. These significant differences between RMD values are mainly due to the selection of the statistical parameters that in turn define the breach parameters when a Monte Carlo approach is used.

This means that studying and defining the breach parameters of the hydraulic model in HEC-RAS in the best possible way is not enough, and the definition of the statistical parameters should also be a focus of analysis. These findings have significant implications in the operational dimension, regardless of the sophistication of the hydraulic model used. Among these implications are the estimated risks associated with the breach, flood zone determination, scaling of projects and the preparation of emergency action plans (EAP). In the case of this study site, for the same distribution function and an exceedance probability of 99%, the RMD values ranged from 6000 m^3/s to 17,000 m^3/s. The variations in the flow magnitudes indicated above directly affect the analysis of the breach hydrograph, which conditions the flood downstream, affecting the wave travel time, the depths and velocities, and thus the flooded areas.

For the sensitivity analyzes of all the simulated scenarios, it was possible to establish that the most influential breach parameter in the generation of the RMD corresponds to the breach formation time (tf), which showed magnitudes much higher than the rest of the parameters in both its standard deviation and the MLR coefficient. Therefore, since tf is the most heavily weighted breach parameter in the RMD calculation, its accurate determination is essential. Secondly, the breach parameters Inv and B have a significant degree of sensitivity. The parameter Inv is more influential on average than B, so the numerical definition should also be considered an essential focus of analysis. The variations produced by the rest of the parameters (LSS, RSS, Init and Cd) are not significant as they have minimal impact on the RMD.

After understanding the influence of the parameters tf, Inv and B, it was possible to corroborate what was expected for the proportionality of these breach parameters with respect to the breach flow generated, where the parameters tf and Inv behave in an inversely proportional manner, and parameter B is directly proportional to the variation of the RMD. Therefore, based on the above, the highest flow for any exceedance probability is associated with the scenario with the lowest mean and standard deviation for tf and Inv, the highest mean and standard deviation for B, and vice versa.

Finally, it should be noted that the conclusions established in this investigation are specific to the study site analyzed, corresponding to the Chacrillas Reservoir. However, the

methodology could be adapted and replicated in other reservoirs of interest, and thus determine whether the behavior is similar to that presented in this study. In the future, it would also be advantageous to compile sensitivity analyses of breach parameters for different dams to relate the variability of the influence of these breach parameters with respect to the characteristics of each study site (e.g., valley slope, wall height, available reservoir volume, roughness, among others). Finally, with respect to the probability density functions and the statistical parameters that are used for probabilistic analysis, it is important to add and work with other density functions than those already available in McBreach.

Supplementary Materials: The following supporting information can be downloaded at https://www.mdpi.com/article/10.3390/w14111776/s1. Table S1: Combinations of statistical parameters. Table S2: Combinations of statistical and deterministic parameters. Table S3: Combinations of breach parameters.

Author Contributions: Conceptualization, H.A. and D.C.; software, D.B.; formal analysis, D.B.; writing—original draft preparation, review and editing, D.B., D.C., H.A. and A.P. All authors have read and agreed to the published version of the manuscript.

Funding: This research was partially funded by Universidad Diego Portales through the internal project "Bridge Erosion Critical Modelling" (grant No. 1100327026), and the project ANID InES Ciencia Abierta INCA210005.

Institutional Review Board Statement: Not applicable.

Informed Consent Statement: Not applicable.

Acknowledgments: Hydraulic Works Department of Chile (Dirección de Obras Hidráulicas MOP) and the project ANID InES Ciencia Abierta INCA210005.

Conflicts of Interest: The authors declare no conflict of interest.

References

1. Álvarez, M.; Puertas, J.; Peña, E.; Bermúdez, M. Two-Dimensional Dam-Break Flood Analysis in Data-Scarce Regions: The Case Study of Chipembe Dam, Mozambique. *Water* **2017**, *9*, 432. [CrossRef]
2. Xu, Y.; Zhang, L.; Jia, J. Lessons from catastrophic dam failures in August 1975 in Zhumadian, China. In Proceedings of the Geosustainability and Geohazard Mitigation, New Orleans, LA, USA, 9–12 March 2008; pp. 162–169. [CrossRef]
3. FEMA. *Fedearl Guidelines for Inundation Mapping of Flood Risks Associated with Dam Incidents and Failures*, 5th ed.; FEMA P-946/July 2013; Technical Report Federal Emergency Management Agency: Washington, DC, USA, 2013.
4. Dhiman, S.; Patra, K.C. Experimental study of embankment breach based on its construction parameters. *Nat. Hazards Earth Syst. Sci. Discuss.* **2017**, *2017*, 1–16. [CrossRef]
5. Godell, C.; Johnson, D.; Raeburn, R.; Monk, S.; Karki, A.; Lee, A. Probabilistic dam breach modelling using HEC-RAS and McBreach; United States Society on Dams. In Proceedings of the 38th Annual Conference and Exhibition, Miami, FL, USA, 4 April 2018.
6. Basheer, T.A.; Wayayok, A.; Yusuf, B.; Kamal, R. Dam breach parameters and their influence on flood hydrographs for mosul dam. *J. Eng. Sci. Technol.* **2017**, *12*, 2896–2908.
7. Wahl, T.L. Uncertainty of Predictions of Embankment Dam Breach Parameters. *J. Hydraul. Eng.* **2004**, *130*, 389–397. [CrossRef]
8. Kirkpatrick, G.W. Evaluation guidelines for spillway adequacy. The evaluation of dam safety. In Proceedings of the Engineering Foundation Conference ASCE, New York, NY, USA, 2–5 May 1977; pp. 395–414.
9. U.S. Bureau of Reclamation. *Guidelines for Defining Inundated Areas Downstream from Bureau of Reclamation Dams*; Reclamation Planning Instruction Report No. 82-11; U.S. Bureau of Reclamation: Washington, DC, USA, 1982.
10. Singh, K.P.; Snorrason, A. Sensitivity of outflow peaks and flood stages to the selection of dam breach parameters and simulation models. *J. Hydrol.* **1984**, *68*, 295–310. [CrossRef]
11. Froehlich, D.C. Peak Outflow from Breached Embankment Dam. *J. Water Resour. Plan. Manag.* **1995**, *121*, 90–97. [CrossRef]
12. Macdonald, T.C.; Langridge-Monopolis, J. Breaching Characteristics of Dam Failures. *J. Hydraul. Eng.* **1984**, *110*, 567–586. [CrossRef]
13. Pierce, M.W.; Thornton, C.I.; Asce, M.; Abt, S.R.; Asce, F. Predicting Peak Outflow from Breached Embankment Dams. *J. Hydrol. Eng.* **2010**, *15*, 338–349. [CrossRef]
14. Gaagai, A.; Aouissi, H.A.; Krauklis, A.E.; Burlakovs, J.; Athamena, A.; Zekker, I.; Boudoukha, A.; Benaabidate, L.; Chenchouni, H. Modeling and Risk Analysis of Dam-Break Flooding in a Semi-Arid Montane Watershed: A Case Study of the Yabous Dam, Northeastern Algeria. *Water* **2022**, *14*, 767. [CrossRef]

15. Wahl, T.L. *Prediction of Embankment Dam Breach Parameters a Literature Review and Needs Assessment*; Dam Safety Research Report; Bureau of Reclamation Dam Safety Office, U.S. Department of Interior: Washington, DC, USA, 1998. Available online: https://www.nrc.gov/docs/ML0901/ML090150051.pdf (accessed on 6 May 2021).
16. Tsai, C.W.; Yeh, J.-J.; Huang, C.-H. Development of probabilistic inundation mapping for dam failure induced floods. *Stoch. Hydrol. Hydraul.* **2019**, *33*, 91–110. [CrossRef]
17. Moglen, G.E.; Hood, K.; Hromadka, T.V. Examination of Multiple Predictive Approaches for Estimating Dam Breach Peak Discharges. *J. Hydrol. Eng.* **2019**, *24*, 04018065. [CrossRef]
18. Goodell, C. An Approach to Dam Breach Modeling. In Proceedings of the FloodRisk 2012 Conference, Rotterdam, The Netherlands, 20–22 November 2012. [CrossRef]
19. Dirección General de Obras Hidráulicas y Calidad de Aguas. *Guía Técnica para la Elaboración de los Planes de Emergencia de Presas*; Ministerio del Medio Ambiente España: Madrid, Spanish, 2021. Available online: https://www.miteco.gob.es/es/agua/publicaciones/ (accessed on 26 May 2021). (In Spanish)
20. Zhou, X.; Zhou, J.; Du, X.; Li, S. Study on dam risk classification in China. *Water Supply* **2014**, *15*, 483–489. [CrossRef]
21. Bello, D.; Alcayaga, H.; Caamaño, D. *Modelación Hidráulica de Rotura del Embalse Chacrillas y Evaluación de la Amenaza Asociada*; Repositorio UDP; Universidad Diego Portales: Santiago, Chile, 2020.
22. USACE. *HEC-RAS Hydraulic Reference Manual*; Version 6.0; U.S. Army Corps of Engineers, Hydrologic Engineering Center: Davis, CA, USA, 2020. Available online: https://www.hec.usace.army.mil/publications/ (accessed on 26 May 2021).
23. Kleinschmidt. Probabilistic Dam Breach Modeling User's Manual—McBreach. 2019. Available online: https://www.kleinschmidtgroup.com/mcbreach/ (accessed on 26 May 2021).
24. International Commission on Large Dams. World Register of Dams. 2011. Available online: http://www.icold-cigb.org (accessed on 22 February 2020).
25. Bellos, V.; Tsakiris, V.K.; Kopsiaftis, G.; Tsakiris, G. Propagating Dam Breach Parametric Uncertainty in a River Reach Using the HEC-RAS Software. *Hydrology* **2020**, *7*, 72. [CrossRef]
26. Yanmaz, A.M.; Gunindi, M.E. Assessment of overtopping reliability and benefits of a flood detention dam. *Can. J. Civ. Eng.* **2008**, *35*, 1177–1182. [CrossRef]
27. Peter, S.J.; Siviglia, A.; Nagel, J.; Marelli, S.; Boes, R.M.; Vetsch, D.; Sudret, B. Development of Probabilistic Dam Breach Model Using Bayesian Inference. *Water Resour. Res.* **2018**, *54*, 4376–4400. [CrossRef]
28. Ahmadisharaf, E.; Kalyanapu, A.J.; Thames, B.A.; Lillywhite, J. A probabilistic framework for comparison of dam breach parameters and outflow hydrograph generated by different empirical prediction methods. *Environ. Model. Softw.* **2016**, *86*, 248–263. [CrossRef]
29. Janke, J.R.; Ng, S.; Bellisario, A. An inventory and estimate of water stored in firn fields, glaciers, debris-covered glaciers, and rock glaciers in the Aconcagua River Basin, Chile, Geomorphology. *Geomorphology* **2017**, *296*, 142–152. [CrossRef]
30. Saltelli, A.; Ratto, M.; Campolongo, F.; Cariboni, J.; Gatelli, D.; Saisana, M.; Tarantola, S. (Eds.) Methods and Settings for Sensitivity Analysis—An Introduction. In *Global Sensitivity Analysis. The Primer*; John Wiley & Sons, Ltda: Hoboken, NJ, USA, 2008; pp. 16–23.
31. Seabold, S.; Perktold, J. Statsmodels: Econometric and Statistical Modeling with Python. In Proceedings of the 9th Python in Science Conference, Austin, TX, USA, 28 June–3 July 2010; pp. 92–96. [CrossRef]